

## Role of the Azadithiolate Cofactor in Models for [FeFe]-Hydrogenase: Novel Structures and Catalytic Implications

Matthew T. Olsen, Thomas B. Rauchfuss,\* and Scott R. Wilson

Department of Chemistry, University of Illinois at Urbana–Champaign,  
Urbana, Illinois 61801, United States

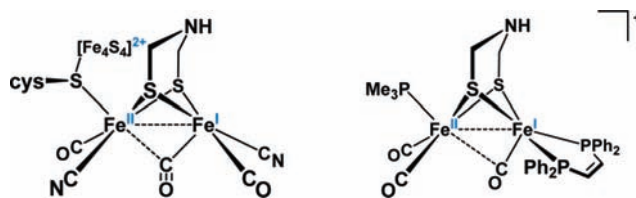
Received May 15, 2010; E-mail: rauchfuz@illinois.edu

**Abstract:** This paper summarizes studies on the redox behavior of synthetic models for the [FeFe]-hydrogenases, consisting of diiron dithiolato carbonyl complexes bearing the amine cofactor and its *N*-benzyl derivative. Of specific interest are the causes of the low reactivity of oxidized models toward H<sub>2</sub>, which contrasts with the high activity of these enzymes for H<sub>2</sub> oxidation. The redox and acid–base properties of the model complexes [Fe<sub>2</sub>[(SCH<sub>2</sub>)<sub>2</sub>NR](CO)<sub>3</sub>(dppv)(PMe<sub>3</sub>)]<sup>+</sup> ([2]<sup>+</sup> for R = H and [2']<sup>+</sup> for R = CH<sub>2</sub>C<sub>6</sub>H<sub>5</sub>, dppv = *cis*-1,2-bis(diphenylphosphino)ethylene) indicate that addition of H<sub>2</sub> followed by deprotonation are (i) endothermic for the mixed valence (Fe<sup>II</sup>Fe<sup>I</sup>) state and (ii) exothermic for the diferrous (Fe<sup>II</sup>Fe<sup>II</sup>) state. The diferrous state is shown to be unstable with respect to coordination of the amine to Fe, a derivative of which was characterized crystallographically. The redox and acid–base properties for the mixed valence models differ strongly for those containing the amine cofactor versus those derived from propanedithiolate. Protonation of [2]<sup>+</sup> induces disproportionation to a 1:1 mixture of the ammonium [H2]<sup>+</sup> (Fe<sup>I</sup>Fe<sup>I</sup>) and the dication [2']<sup>2+</sup> (Fe<sup>II</sup>Fe<sup>II</sup>). This effect is consistent with substantial enhancement of the basicity of the amine in the Fe<sup>I</sup>Fe<sup>I</sup> state vs the Fe<sup>II</sup>Fe<sup>I</sup> state. The Fe<sup>I</sup>Fe<sup>I</sup> ammonium compounds are rapid and efficient H-atom donors toward the nitroxyl compound TEMPO. The atom transfer is proposed to proceed via the hydride. Collectively, the results suggest that proton-coupled electron-transfer pathways should be considered for H<sub>2</sub> activation by the [FeFe]-hydrogenases.

### Introduction

The catalytic chemistry of hydrogen evolution and oxidation is topical because H<sub>2</sub> is a versatile reagent and a promising carrier of energy.<sup>1,2</sup> New approaches to this area of catalysis have been inspired by the hydrogenase enzymes, and studies on the [FeFe]-hydrogenases have proven especially influential.<sup>3</sup> We and others have proposed that catalysis occurs at a single coordination site on one Fe center of the diiron subunit (Figure 1),<sup>4,5</sup> with participation of various cofactors.

Ongoing research in this area focuses on elucidating the electronic features of the bimetallic site (oxidation state, redox

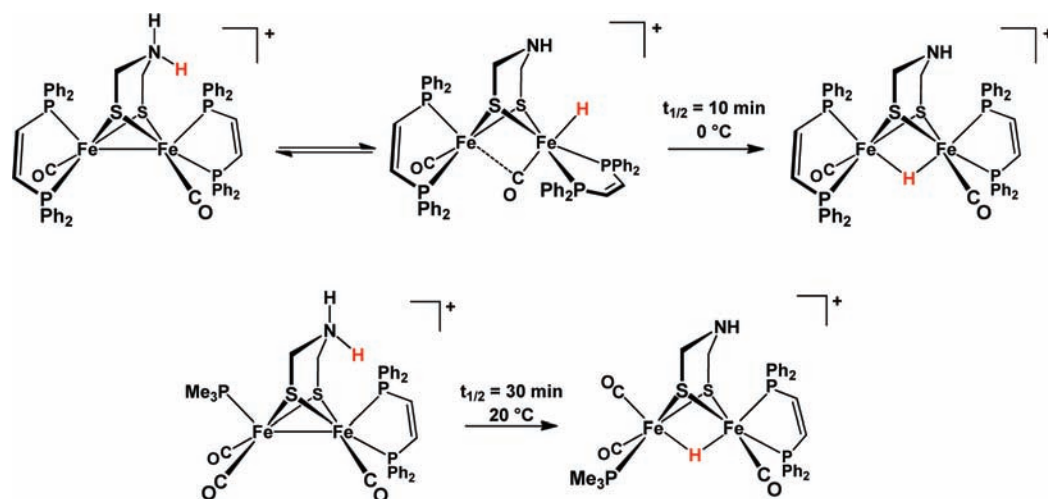


**Figure 1.** Active site of the oxidized state (H<sub>ox</sub>) of the [FeFe]-hydrogenase (left),<sup>7,8</sup> showing the azadithiolate cofactor and a vacant site on the distal iron center.<sup>9</sup> Model complex for the H<sub>ox</sub> state of the active site (right), with organophosphorus ligands in place of the cyanide and 4Fe–4S cofactors.

potentials, asymmetry) and equipping models with the cofactors required for efficient catalysis. Thus, models have evolved from the simple Fe<sub>2</sub>(SR)<sub>2</sub>(CO)<sub>6</sub> to substituted derivatives Fe<sub>2</sub>(SR)<sub>2</sub>(CO)<sub>6-x</sub>L<sub>x</sub>, which exhibit the two essential attributes of hydrogenases, acid–base and redox behavior. Two cofactors are of functional significance since they enhance the redox or acid–base properties inherent in the diiron center. First, the redox-active 4Fe–4S cluster allows the diiron subsite, which operates via a 1e<sup>-</sup> couple, to effect 2e<sup>-</sup> redox reactions, as required by the H<sub>2</sub>/2H<sup>+</sup> redox couple. Second, and very relevant to this report, the amine-containing dithiolate cofactor<sup>4,5</sup> is proposed to relay protons to and from the distal Fe.<sup>6</sup>

Synthetic models differ from the diiron site in the protein in three important ways. First, most models feature organophosphorus ligands such as *cis*-1,2-C<sub>2</sub>H<sub>2</sub>(PPh<sub>2</sub>)<sub>2</sub> (dppv) and PMe<sub>3</sub> in place of the cyanide cofactors. This change enables

- (1) Kubas, G. J. *Metal Dihydrogen and  $\sigma$ -Bond Complexes*; Kluwer Academic/Plenum: New York, 2001.
- (2) Vincent, K. A.; Parkin, A.; Armstrong, F. A. *Chem. Rev.* **2007**, *107*, 4366–4413.
- (3) Rakowski DuBois, M.; DuBois, D. L. *Chem. Soc. Rev.* **2009**, *38*, 62–72.
- (4) Lubitz, W.; Reijerse, E.; van Gestel, M. *Chem. Rev.* **2007**, *107*, 4331–4365.
- (5) Silakov, A.; Wenk, B.; Reijerse, E. J.; Lubitz, W. *Phys. Chem. Chem. Phys.* **2009**, *11*, 6592–6599.
- (6) Barton, B. E.; Olsen, M. T.; Rauchfuss, T. B. *J. Am. Chem. Soc.* **2008**, *130*, 16834–16835.
- (7) Peters, J. W.; Lanzilotta, W. N.; Lemon, B. J.; Seefeldt, L. C. *Science* **1998**, *282*, 1853–1858.
- (8) Nicolet, Y.; de Lacey, A. L.; Vernede, X.; Fernandez, V. M.; Hatchikian, E. C.; Fontecilla-Camps, J. C. *J. Am. Chem. Soc.* **2001**, *123*, 1596–1601.
- (9) Olsen, M. T.; Barton, B. E.; Rauchfuss, T. B. *Inorg. Chem.* **2009**, *48*, 7507–7509.

Scheme 1. Regiochemistry of Protonation of Tri- and Tetrasubstituted Diiron Azadithiolato Carbonyl Complexes<sup>6,9</sup>

mechanistic studies without the complications of reactions at FeCN. Second, with a single exception,<sup>10</sup> models omit the 4Fe–4S cofactor that is found in the 6-Fe “H-cluster” (Figure 1). Finally, the model complexes differ from the active site in the stereochemistry of one of the iron centers. In the protein, the distal Fe center adopts an “inverted” (also described as “rotated”<sup>11</sup>) structure in which a CO ligand occupies a semibridging position between the two Fe centers. This stereochemistry exposes a coordination site adjacent to the amine of the dithiolate cofactor. The inverted structure is observed in the *oxidized* models of the type  $[\text{Fe}_2(\text{SR})_2(\text{CO})_4\text{L}_2]^+$  and  $[\text{Fe}_2(\text{SR})_2(\text{CO})_3\text{L}_3]^+$ ,<sup>12–15</sup> but such inverted structures are rarely observed in *reduced* diiron models.<sup>16,17</sup> Theoretical studies indicate that rotated structures are destabilized by about 10 kcal in model complexes.<sup>11</sup>

More recent models incorporate the amine cofactor, which we call azadithiolate ( $\text{adt} = (\text{SCH}_2)_2\text{NH}^{2-}$ ). *N*-Protonation of such compounds shifts the reduction potential of the diiron center by  $\sim 0.5$  V and the oxidation potential by  $\sim 0.2$  V.<sup>18,19</sup> Of relevance to the enzymatic mechanism, the complex  $\text{Fe}_2(\text{adt})(\text{CO})_2(\text{dppv})_2$  electrocatalyzes hydrogen evolution from weaker acids than is possible for the related complexes lacking the amine, for example,  $\text{Fe}_2(\text{pdt})(\text{CO})_2(\text{dppv})_2$  ( $\text{pdt} = \text{S}_2(\text{CH}_2)_3^{2-}$ ).<sup>6</sup> Catalysis by these electron-rich models proceeds via the intermediacy of an iron hydride, for which the rates of formation and deprotonation are modified by the

amine. Such amine-complemented models for the  $\text{H}_{\text{ox}}$  state are ideal systems to explore factors relevant to  $\text{H}_2$  oxidation. In the present report, we examine the interplay between the acid–base behavior of the amine and the redox properties of the  $\text{Fe}_2$  centers in  $\text{Fe}_2(\text{adt})(\text{CO})_3(\text{dppv})(\text{PMe}_3)$ .<sup>9</sup> Protonation of  $\text{Fe}_2(\text{adt})(\text{CO})_3(\text{dppv})(\text{PMe}_3)$  gives the ammonium derivative as the only spectroscopically detectable tautomer. Via a first-order pathway, the ammonium compound tautomerizes slowly at room temperature in  $\text{CH}_2\text{Cl}_2$  solution to the isomeric “ $\mu$ -hydride”, which features  $\text{H}^-$  bound to both Fe centers (Scheme 1).<sup>9,20</sup>

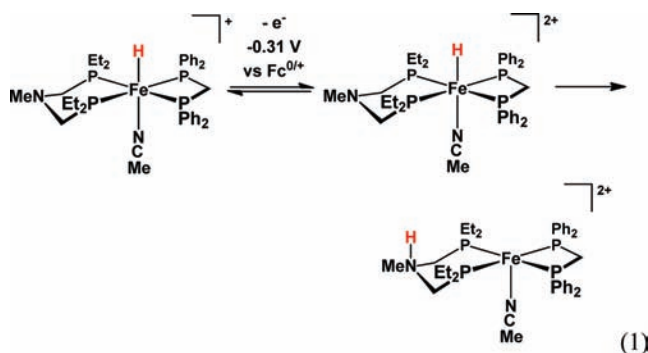
In contrast to the “trisphosphine” discussed above, the tetrasubstituted diiron dithiolates form spectroscopically detectable terminal hydrides. The enzyme is thought to operate via such terminal hydrides (indicated as *t*-H), not  $\mu$ -hydrides. For  $[(t\text{-H})\text{Fe}_2(\text{adt})(\text{CO})_2(\text{dppv})_2]\text{BF}_4$ , the  $\text{p}K_{\text{a}}^{\text{CDCl}_2}$  is between 5.7 and 8.2.<sup>6</sup> The terminal hydride and ammonium tautomers of this complex coexist in comparable amounts in  $\text{CH}_2\text{Cl}_2$  solution (Scheme 1). Indicative of the subtleties of this system is the finding that high concentrations of  $\text{BF}_4^-$  shift the equilibrium from the hydride toward the ammonium tautomer.<sup>6</sup>

The process by which  $\text{H}_2$  is activated by diiron dithiolato complexes came into focus with the finding that  $\text{H}_2$  is only slowly oxidized by  $[\text{Fe}_2(\text{adt})(\text{CO})_3(\text{dppv})(\text{PMe}_3)]^+$  (at 1800 psi  $\text{H}_2$ , rate  $\approx 10^{-4} \text{ s}^{-1}$ ),<sup>9</sup> whereas the enzyme from *Desulfovibrio gigas* oxidizes  $\text{H}_2$  at  $10^5 \text{ s}^{-1}$ .<sup>21</sup> The low reactivity of mixed valence models toward  $\text{H}_2$  is generally understandable because the heterolytic scission of  $\text{H}_2$  by iron characteristically requires ferrous centers.<sup>1</sup> Theoretical studies show that the diferrous state of the diiron subsite is well suited for activation of  $\text{H}_2$ .<sup>22</sup> Diferrous  $\mu$ -hydride complexes catalyze H–D exchange between  $\text{H}_2$  and  $\text{D}_2\text{O}$ , albeit only photochemically.<sup>23</sup> Diferrous compounds that contain a vacant coordination site are rare,<sup>24,25</sup> but unsaturated mononuclear ferrous complexes have much precedence and often

- (10) Tard, C.; Liu, X.; Ibrahim, S. K.; Bruschi, M.; De Gioia, L.; Davies, S. C.; Yang, X.; Wang, L.-S.; Sawers, G.; Pickett, C. J. *Nature* **2005**, *433*, 610–614.
- (11) Tye, J. W.; Darensbourg, M. Y.; Hall, M. B. *Inorg. Chem.* **2006**, *45*, 1552–1559.
- (12) Justice, A. K.; Rauchfuss, T. B.; Wilson, S. R. *Angew. Chem., Int. Ed.* **2007**, *46*, 6152–6154.
- (13) Justice, A. K.; De Gioia, L.; Nilges, M. J.; Rauchfuss, T. B.; Wilson, S. R.; Zampella, G. *Inorg. Chem.* **2008**, *47*, 7405–7414.
- (14) Liu, T.; Darensbourg, M. Y. *J. Am. Chem. Soc.* **2007**, *129*, 7008–7009.
- (15) Thomas, C. M.; Liu, T.; Hall, M. B.; Darensbourg, M. Y. *Inorg. Chem.* **2008**, *47*, 7009–7024.
- (16) Olsen, M. T.; Bruschi, M.; De Gioia, L.; Rauchfuss, T. B.; Wilson, S. R. *J. Am. Chem. Soc.* **2008**, *130*, 12021–12030.
- (17) Cheah, M. H.; Tard, C.; Borg, S. J.; Liu, X.; Ibrahim, S. K.; Pickett, C. J.; Best, S. P. *J. Am. Chem. Soc.* **2007**, *129*, 11085–11092.
- (18) Eilers, G.; Schwartz, L.; Stein, M.; Zampella, G.; De Gioia, L.; Ott, S.; Lomoth, R. *Chem.—Eur. J.* **2007**, *13*, 7075–7084.
- (19) Ezzaher, S.; Orain, P.; Capon, J.; Gloaguen, F.; Petillon, F.; Roisnel, T.; Schollhammer, P.; Talarmin, J. *Chem. Commun.* **2008**, 2547, 2549.

- (20) Barton, B. E.; Zampella, G.; Justice, A. K.; De Gioia, L.; Rauchfuss, T. B.; Wilson, S. R. *Dalton Trans.* **2010**, 3011–3019.
- (21) Fontecilla-Camps, J. C.; Volbeda, A.; Cavazza, C.; Nicolet, Y. *Chem. Rev.* **2007**, *107*, 4273–4303.
- (22) Siegbahn, P. E. M.; Tye, J. W.; Hall, M. B. *Chem. Rev.* **2007**, *107*, 4414–4435.
- (23) Zhao, X.; Chiang, C.-Y.; Miller, M. L.; Rampersad, M. V.; Darensbourg, M. Y. *J. Am. Chem. Soc.* **2003**, *125*, 518–524.

form  $\eta^2$ -H<sub>2</sub> complexes.<sup>26,27</sup> Furthermore, amine-complemented mononuclear ferrous phosphine complexes have been shown to undergo redox-triggered tautomerization (eq 1).<sup>28</sup>



## Results

**Synthesis and Characterization of Diferrous  $\kappa^3$ -Azadithiolato Complexes.** On a preparative scale and consistent with ample precedent,<sup>12–15</sup> oxidation of Fe<sub>2</sub>[(S(CH<sub>2</sub>)<sub>2</sub>X)(CO)<sub>3</sub>(dppv)(PMe<sub>3</sub>)] with Fc<sup>+</sup> was found to yield the mixed valence Fe<sup>II</sup>Fe<sup>I</sup> derivatives (“H<sub>ox</sub> models”), where X = CH<sub>2</sub>, NH, NBn, and O, for **1**, **2**, **2'**, and **3**, respectively (Bn = CH<sub>2</sub>C<sub>6</sub>H<sub>5</sub>).<sup>9,12</sup> These cationic derivatives were isolated using bulky arylborate counteranions, which are essential for the stabilization of H<sub>ox</sub> models.<sup>9</sup> The azadithiolates were found to undergo a second oxidation with FcBAR<sup>F</sup><sub>4</sub>, and in this way we generated [2'](BAR<sup>F</sup><sub>4</sub>)<sub>2</sub> (FcBAR<sup>F</sup><sub>4</sub> = [Fe(C<sub>5</sub>H<sub>5</sub>)<sub>2</sub>]B(C<sub>6</sub>H<sub>3</sub>-3,5-(CF<sub>3</sub>)<sub>2</sub>)<sub>4</sub>). The initial <sup>31</sup>P NMR spectrum at –70 °C indicates that [2'](BAR<sup>F</sup><sub>4</sub>)<sub>2</sub> is diamagnetic and C<sub>s</sub>-symmetric. In FTIR spectra of solutions of [2'](BAR<sup>F</sup><sub>4</sub>)<sub>2</sub>, the  $\nu_{CO}$  bands are shifted to higher energy by ~40 cm<sup>-1</sup> from the positions for [2']<sup>+</sup>, and all three bands occur in the terminal carbonyl region (2066, 2008, and 1977 cm<sup>-1</sup>). When we instead employed the oxidant FcBF<sub>4</sub>, a spectroscopically distinct compound was observed (Supporting Information).

Treatment of a CD<sub>2</sub>Cl<sub>2</sub> solution of [2']<sup>2+</sup> with MeCN was found to afford stable adducts, regardless of the counteranion, of the formula [2'(MeCN)]<sup>2+</sup>. Although the BAR<sup>F</sup><sub>4</sub><sup>-</sup> salts afforded tacky oils, the BF<sub>4</sub><sup>-</sup> salts readily crystallized. The crystallographic analysis of this salt revealed a diiron dithiolate as expected, but unlike all previously reported azadithiolato complexes,<sup>29–31</sup> the amine is coordinated to Fe (Figure 2). The Fe···Fe distance of 3.447(2) Å is nonbonding, which is also uncommon.<sup>24,32–34</sup> The two iron centers, which are still linked

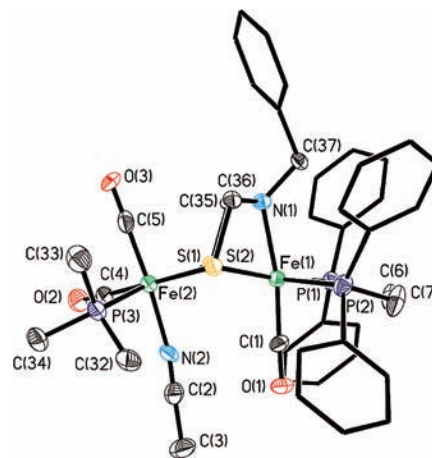


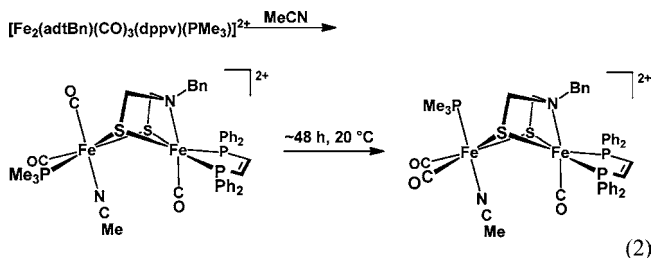
**Figure 2.** Structure of the dication in [2'(MeCN)](BF<sub>4</sub>)<sub>2</sub>. Thermal ellipsoids set at the 30% probability level and hydrogen atoms are not shown.

**Table 1.** Selected Bond Distances (Å) and Angles (deg) for [2'(MeCN)](BF<sub>4</sub>)<sub>2</sub>

bond	distance	bonds	angles
Fe(1)–N(1)	2.098(8)	N(1)–Fe(1)–S(2)	72.9(2)
Fe(1)–Fe(2)	3.477(2)	Fe(1)–S(2)–C(36)	80.9(3)
Fe(1)–C(1)	1.753(11)	Fe(2)–S(2)–C(36)	107.7(4)
Fe(2)–N(2)	1.965(10)	S(1)–Fe(1)–S(2)	80.97(11)
Fe(1)–S(2)	2.336(3)	S(1)–Fe(2)–S(2)	81.45(11)
Fe(2)–S(2)	2.323(3)	P(1)–Fe(1)–P(2)	87.24(12)

by a pair of thiolates, are each octahedral. The coordination spheres of the Fe subsites are described as Fe(CO)<sub>2</sub>(PMe<sub>3</sub>)-(MeCN)(SR)<sub>2</sub> and Fe(CO)(dppv)(amine)(SR)<sub>2</sub>. The S–Fe–N angles are acute at ~73°, but the other Fe–ligand bond lengths and angles are within the normal range (Table 1).

The solution properties of [2'(MeCN)]<sup>2+</sup> were examined by variable-temperature <sup>31</sup>P NMR spectroscopy. Dissolution of the crystalline [2'(MeCN)](BF<sub>4</sub>)<sub>2</sub> at –70 °C gave a compound with the same spectroscopic signature as that obtained by addition of MeCN to a CD<sub>2</sub>Cl<sub>2</sub> solution of [2'](BAR<sup>F</sup><sub>4</sub>)<sub>2</sub> generated at –70 °C. Over the course of ~24 h at 20 °C, this species isomerized to a second symmetrical isomer (two <sup>31</sup>P NMR signals) (eq 2, Figure 3). Solutions of [2'](BAR<sup>F</sup><sub>4</sub>)<sub>2</sub> were found to rapidly and irreversibly form an adduct upon treatment with 1 atm of CO. In contrast, monocation [2']<sup>+</sup> binds CO reversibly, and the adducts are only observable at low temperatures.<sup>9,13</sup> Treatment of [2'](BAR<sup>F</sup><sub>4</sub>)<sub>2</sub> with 1800 psi H<sub>2</sub> for 30 h gave [2'(μ-H)]<sup>+</sup> as well as smaller amounts of [Fe(H)(CO)<sub>3</sub>(dppv)]<sup>+</sup>. Additionally, [2']<sup>2+</sup> was found to react at low temperatures with PhSiH<sub>3</sub> to give the hydride [2'(μ-H)]<sup>+</sup>.



**Electrochemical Properties of Diiron Azadithiolates.** Diiron dithiolates of the formula Fe<sub>2</sub>[(S(CH<sub>2</sub>)<sub>2</sub>X)(CO)<sub>3</sub>(dppv)(PMe<sub>3</sub>)] undergo a reversible 1e<sup>-</sup> oxidation for X = CH<sub>2</sub>, NH, NCH<sub>2</sub>C<sub>6</sub>H<sub>5</sub>, and O (for **1**, **2**, **2'**, and **3**; see Figure 4, eq 3, and

- (24) van der Vlugt, J. I.; Rauchfuss, T. B.; Wilson, S. R. *Chem.—Eur. J.* **2005**, *12*, 90–98.  
 (25) Justice, A. K.; Nilges, M. J.; Rauchfuss, T. B.; Wilson, S. R.; De Gioia, L.; Zampella, G. *J. Am. Chem. Soc.* **2008**, *130*, 5293–5301.  
 (26) Kubas, G. J. *Chem. Rev.* **2007**, *107*, 4152–4205.  
 (27) Landau, S. E.; Morris, R. H.; Lough, A. J. *Inorg. Chem.* **1999**, *38*, 6060–6068.  
 (28) Henry, R. M.; Shoemaker, R. K.; Dubois, D. L.; Rakowski DuBois, M. *J. Am. Chem. Soc.* **2006**, *128*, 3002–3010.  
 (29) Lawrence, J. D.; Li, H.; Rauchfuss, T. B.; Bénard, M.; Rohmer, M.-M. *Angew. Chem., Int. Ed.* **2001**, *40*, 1768–1771.  
 (30) Ott, S.; Kritikos, M.; Åkermark, B.; Sun, L.; Lomoth, R. *Angew. Chem., Int. Ed.* **2004**, *43*, 1006–1009.  
 (31) Dong, W.; Wang, M.; Liu, X.; Jin, K.; Li, G.; Wang, F.; Sun, L. *Chem. Commun.* **2006**, 305–307.



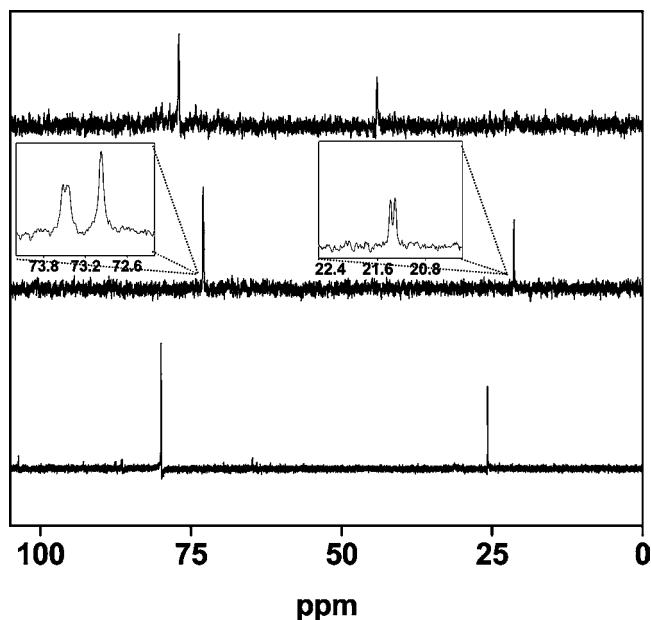


**Figure 3.**  $^{31}\text{P}$  NMR spectra ( $\text{CD}_2\text{Cl}_2$ ) of a fresh solution of  $[\mathbf{2}'](\text{BARF}_4)_2$  at  $-193\text{ K}$  (top), after treatment with  $\text{CD}_3\text{CN}$  (middle), and after allowing the same solution to stand at  $293\text{ K}$  for 48 h. Signals at  $>70$  are assigned to dppv and those absorbing at  $<40$  are assigned to  $\text{PMe}_3$ .

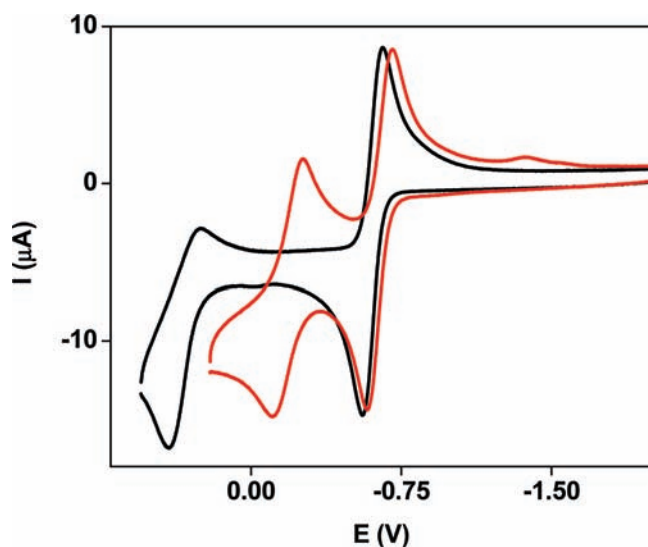
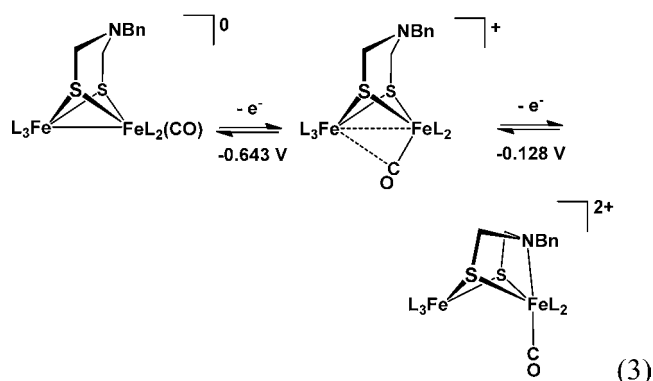


**Figure 4.** Cyclic voltammograms of a  $\text{CH}_2\text{Cl}_2$  solution of  $\mathbf{1}$  (black) and  $\mathbf{2}'$  (red) illustrative of the effect of the azadithiolate on the second anodic event. Conditions:  $0.001\text{ M } \mathbf{2}'$ ,  $0.300\text{ M } [(\text{C}_4\text{H}_9)_4\text{N}]\text{PF}_6$ ,  $\text{CH}_2\text{Cl}_2$ ,  $20\text{ }^\circ\text{C}$ ,  $0.1\text{ V/s}$  scan rate.

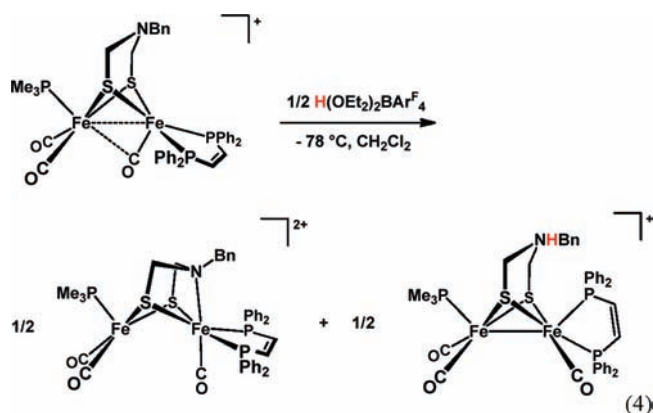
Table 2). For  $\mathbf{2}'$ , the ratios of the oxidation and reduction currents ( $i_{\text{pc}}/i_{\text{pa}}$ ) are  $>0.9$  at a scan rate of  $0.100\text{ V/s}$  in noncoordinating solvents ( $\text{CH}_2\text{Cl}_2$ ). The linear dependence of  $i_{\text{p}}$  on (scan rate) $^{0.5}$  also indicates a diffusion-controlled process.

Oxidations corresponding to the  $[\text{Fe}_2(\text{SR})_2]^{+/2+}$  ( $\text{Fe}^{\text{II}}\text{Fe}^{\text{I}}/\text{Fe}^{\text{II}}\text{Fe}^{\text{II}}$ ) couple proved highly dependent on the dithiolate (Figure 4 and eq 3). For the propane- and oxadithiolato compounds, but not the azadithiolates, a poorly reversible second oxidation is observed at  $0.890 \pm 0.040\text{ V}$  more anodic than the  $[\text{Fe}_2(\text{SR})_2]^{0/+}$  couple. Unlike the amine-free derivatives, the  $[\text{Fe}_2(\text{SR})_2]^{+/2+}$  couple for the azadithiolates  $\mathbf{2}$  and  $\mathbf{2}'$  occurs at mild potentials and displays full reversibility. Interestingly  $\Delta E$  for  $\mathbf{2}$  is significantly smaller than that for  $\mathbf{2}'$ . When noncoordinating  $[(\text{C}_4\text{H}_9)_4\text{N}]\text{BARF}_4$  electrolyte was employed,  $\Delta E$  in-

creased by 130 and 177 mV for  $\mathbf{2}'$  and  $\mathbf{2}$ , respectively. This separation of electrochemical events is commonly observed in noncoordinating electrolytes, $^{35}$  and the larger value of  $\Delta E$  for  $\mathbf{2}$  versus  $\mathbf{2}'$  is attributable to the ability of smaller fluoroanions such as  $\text{PF}_6^-$  to engage in hydrogen-bonding. $^{36}$  Upon addition of MeCN to  $\text{CH}_2\text{Cl}_2$  solutions of  $\mathbf{2}'$ ,  $E_2$  becomes irreversible, and two closely spaced cathodic waves are observed at  $-0.80$  and  $-0.90\text{ V}$ . The strong effect of MeCN is consistent with the formation of the adduct  $[\mathbf{2}'(\text{MeCN})]^{2+}$ .



**Acid–Base Reactions.** The  $\text{p}K_{\text{a}}^{\text{CD}_2\text{Cl}_2}$  values of the ammonium compounds  $[\text{H}_2']^+$  and  $[\text{H}_2]^{2+}$  were measured as 3.3 and 3.2, respectively, by titration of  $\mathbf{2}'$  and  $\mathbf{2}$  with  $[\text{HPMe}_2\text{Ph}]\text{BF}_4$  ( $\text{p}K_{\text{a}}^{\text{CD}_2\text{Cl}_2} = 5.7$ ). $^{37}$  The  $\text{p}K_{\text{a}}^{\text{CH}_3\text{CN}}$  value for  $[\text{H}_2']^+$  was determined to be 13.1 by titration with  $\text{ClCH}_2\text{CO}_2\text{H}$  ( $\text{p}K_{\text{a}}^{\text{CH}_3\text{CN}} = 15.3$ ). We could not directly determine the corresponding  $\text{p}K_{\text{a}}$  of  $[\text{H}_2']^{2+}$  because  $[\mathbf{2}']^+$  undergoes quasi-disproportionation upon treatment with acids, even in solution at  $-78\text{ }^\circ\text{C}$ . The product mixture consists of equal amounts of the reduced ammonium species  $[\text{H}_2']^+$  and the dication  $[\mathbf{2}']^{2+}$  (eq 4, Figure 5).



The proton-induced quasi-disproportionation of  $[\mathbf{2}']^+$  (eq 4) is driven by the strong oxidizing ability of  $[\text{H}_2']^{2+}$ . The requirement of 0.5 equiv of acid for the reaction in eq 2 was confirmed. Furthermore,  $>0.5$  equiv of  $\text{H}(\text{OEt}_2)_2\text{BARF}_4$  was found not to affect the product distribution, a result consistent with the low basicity of  $[\mathbf{2}']^{2+}$ , wherein the amine is coordinated to Fe. In contrast to this behavior, mixed-valence  $\text{Fe}(\text{I})\text{Fe}(\text{II})$  complexes lacking azadithiolates are unreactive toward acid. For example, a  $\text{CH}_2\text{Cl}_2$  solution of  $[\text{Fe}_2(\text{S}_2\text{C}_3\text{H}_6)(\text{CO})_3\text{-}(\text{dppv})(\text{PMe}_3)]\text{BARF}_4$  was unaffected by treatment with  $\text{H}(\text{OEt}_2)_2\text{BARF}_4$  at  $20\text{ }^\circ\text{C}$ .

Together with the  $\text{p}K_{\text{a}}$  for  $[\text{H}_2']^+$ ,  $E_{1/2}$  for the  $[\text{H}_2']^{+/2+}$  couple would allow us to calculate the  $\text{p}K_{\text{a}}$  of the mixed valence ammonium cation  $[\text{H}_2']^{2+}$ . The  $[\text{H}_2']^{+/2+}$  couple is irreversible,

**Table 2.** Half-wave Potentials (V) for the  $[\text{Fe}_2(\text{SR})_2]^{0/+}$  and  $[\text{Fe}_2(\text{SR})_2]^{+/2+}$  Couples for  $\text{Fe}_2[(\text{SCH}_2)_2\text{X}](\text{CO})_3(\text{dppv})(\text{PMe}_3)^{\text{a}}$ 

dithiolate	electrolyte	$E_1$ for $[\text{Fe}_2(\text{SR})_2]^{0/+}$ ( $\Delta E_p$ , V) [ $i_{\text{pc}}/i_{\text{pa}}$ ]	$E_2$ for $[\text{Fe}_2(\text{SR})_2]^{+/2+}$ ( $\Delta E_p$ ) [ $i_{\text{pc}}/i_{\text{pa}}$ ]	$E_2 - E_1$
$(\text{SCH}_2)_2\text{NBn}$ ( <b>2'</b> )	$[(\text{C}_4\text{H}_9)_4\text{N}]\text{PF}_6$	-0.643 (0.118) [ $>0.9$ ]	-0.128 (0.147) [ $>0.9$ ]	0.515
$(\text{SCH}_2)_2\text{NBn}$ ( <b>2'</b> )	$[(\text{C}_4\text{H}_9)_4\text{N}]\text{BARF}_4$	-0.715 (0.111) [0.9]	-0.070 (0.222) [0.7] <sup>c</sup>	0.645
$(\text{SCH}_2)_2\text{NH}$ ( <b>2</b> )	$[(\text{C}_4\text{H}_9)_4\text{N}]\text{PF}_6$	-0.561 (0.095) <sup>b</sup>	-0.363 (0.101) <sup>b</sup>	0.198
$(\text{SCH}_2)_2\text{NH}$ ( <b>2</b> )	$[(\text{C}_4\text{H}_9)_4\text{N}]\text{BARF}_4$	-0.624 (0.075) [ $>0.9$ ]	-0.249 (0.175) [0.1] <sup>c</sup>	0.375
$(\text{SCH}_2)_2\text{CH}_2$ ( <b>1</b> )	$[(\text{C}_4\text{H}_9)_4\text{N}]\text{PF}_6$	-0.609 (0.126) [ $>0.9$ ]	0.356 (0.160) [0.2]	0.965
$(\text{S}_2\text{C}_2\text{H}_4)$	$[(\text{C}_4\text{H}_9)_4\text{N}]\text{PF}_6$	-0.469 (0.121) [ $>0.9$ ]	0.345 (0.143) [0.5]	0.930
$(\text{SCH}_2)_2\text{O}$ ( <b>3</b> )	$[(\text{C}_4\text{H}_9)_4\text{N}]\text{PF}_6$	-0.528 (0.139) [ $>0.9$ ]	0.353 (0.233) [0.1]	0.840
$[(\text{SCH}_2)_2\text{NBn}(\text{H})]^+$ ( $[\text{H}2']^+$ )	$[(\text{C}_4\text{H}_9)_4\text{N}]\text{PF}_6$	$E_{\text{p}2} = 0.040$ (irrev.)		
$[(\text{SCH}_2)_2\text{NH}_2]^+$ ( $[\text{H}2]^+$ )	$[(\text{C}_4\text{H}_9)_4\text{N}]\text{PF}_6$	$E_{\text{p}2} = 0.050$ (irrev.)		

<sup>a</sup> Conditions: 1 mM diiron complex, 100 mM  $[\text{Bu}_4\text{N}]\text{PF}_6$ ,  $\text{CH}_2\text{Cl}_2$  solution, vs  $\text{Fc}^{0/+}$ , 0.1 V/s scan rate. Under our experimental conditions, an internal standard of Fc (1 mM) displayed  $\Delta E_p \approx 100$  mV. The  $i_{\text{pa}}/i_{\text{pc}}$  values for  $E_1$  were recorded under conditions where the scan range did not extend to  $E_2$ .  
<sup>b</sup> The  $i_{\text{pc}}/i_{\text{pa}}$  ratio was not determined. The close separation of the two oxidation steps precludes accurate measurement of this current ratio. <sup>c</sup> At fast scan rates the cathodic return wave of  $E_2$  becomes broadened making the  $i_{\text{pc}}/i_{\text{pa}}$  value an inaccurate representation of reversibility. At slow scan rates,  $E_2$  is fully reversible.

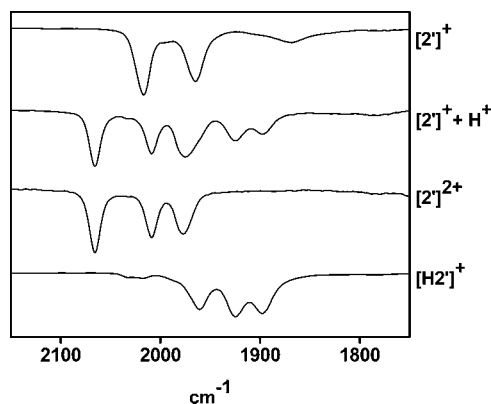
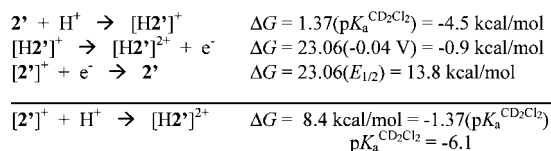


**Figure 5.** IR spectra ( $\text{CH}_2\text{Cl}_2$  solution) for  $[2']^+$  (top), the products of its reaction with 0.5 equiv of  $\text{H}(\text{OEt}_2)_2\text{BARF}_4$  (middle top),  $[2'](\text{BARF}_4)_2$  (middle bottom), and  $[\text{H}2']^+$  generated by protonation of **2'** with  $\text{H}(\text{OEt}_2)_2\text{BARF}_4$  (bottom). Component IR bands ( $\text{CH}_2\text{Cl}_2$ ) are as follows:  $[2']^+$  2017, 1965, 1867  $\text{cm}^{-1}$ ;  $[2']^{2+}$  2065, 2009, 1977;  $[\text{H}2']^+$  1960, 1925, 1898  $\text{cm}^{-1}$ .

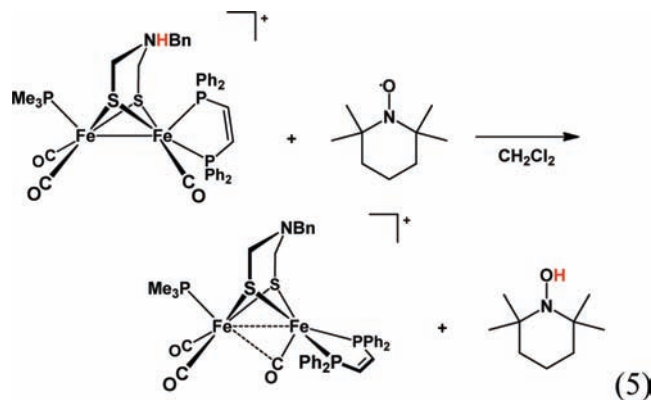
**Scheme 2.** Bordwell Calculation at 20 °C of the  $\text{p}K_a^{\text{CD}_2\text{Cl}_2}$  of  $[\text{H}2']^{2+}$  Assuming  $E_{1/2}$  of the  $[\text{H}2']^{+/2+}$  Couple as 0.04 V



thus precluding accurate determination of  $E_{1/2}$ . Nonetheless, estimating  $E_{1/2}$  as the potential of the anodic wave at half-height would indicate that  $1\text{e}^-$  oxidation of  $[\text{H}2']^+$  decreases the basicity of the amine by as much as  $10^9$  ( $\text{CH}_2\text{Cl}_2$  solution, Scheme 2).

**H-Atom Transfer Reactions.** The electron-rich *N*-protonated azadithiolato complexes were found to serve as H-atom donors. Thus, treatment of  $[\text{H}2']^+$  with 1 equiv of 2,2,6,6-tetramethylpiperidin-1-oxyl (TEMPO), an H-atom abstracting agent,<sup>38</sup> immediately and quantitatively yielded  $[2']^+$  at 293 °C (eq 5,  $\text{R}_2\text{NO} = \text{TEMPO}$ ). This reaction is conveniently monitored by IR spectroscopy in the  $\nu_{\text{CO}}$  region.

When the reaction was monitored by *in situ* IR spectroscopy at low temperatures, a transient build-up of **2'** was detected. This species results from the reversible deprotonation of  $[\text{H}2']^+$  by TEMPOH, the product of eq 5.<sup>39</sup> At 199 K, the rate of disappearance of  $[\text{H}2']^+$  is  $8.13 \times 10^{-3} \text{ s}^{-1} \text{ M}^{-1}$ . By measuring the temperature dependence of the rate constant over the range 199–229 K, we determined that  $\Delta G^\ddagger$  is 13.5 kcal/mol (199 K). The secondary ammonium  $[\text{H}2']^+$  was observed to react with



TEMPO faster than did  $[\text{H}2']^+$  under similar conditions: the reaction was complete in minutes vs  $\sim 60$  min for the Bn derivative at 199 K.

Insights into a possible mechanism of the hydrogen-atom transfer reactions were provided by experiments with the terminal hydrides  $[\text{HFe}_2[(\text{SCH}_2)_2\text{NR}](\text{CO})_2(\text{dppv})_2]^+$  and  $[\text{HFe}_2(\text{pdt})(\text{CO})_2(\text{dppv})_2]^+$ .<sup>6</sup> In  $\text{CH}_2\text{Cl}_2$  solution, both species were found to react ( $t_{1/2} \approx 10$  min, 199 K) with TEMPO to give the corresponding mixed-valence Fe(II)Fe(I) derivatives.<sup>25</sup> The IR signatures for the diferrous hydride starting materials and mixed valence products overlap, thus we conducted these oxidations under an atmosphere of CO, which rapidly affords the CO adducts that display distinctive IR signatures.<sup>25</sup>

## Conclusions

The hydrogenases function by coupling or combining acid–base and redox properties. The present study examined the interplay of these properties in a diiron model that contains both a base and a redox center. We report three unusual findings:

(i) The mildness and reversibility of the  $\text{Fe}^{\text{II}}\text{Fe}^{\text{I}}/\text{Fe}^{\text{II}}\text{Fe}^{\text{II}}$  couple in models containing the amine cofactor arises from the formation of an Fe–N bond. In the absence of the amine,  $32\text{e}^-$  diferrous dithiolates which are analogues of  $[\text{Fe}_2(\text{pdt})(\text{CO})_3(\text{dppv})(\text{PMe}_3)]^{2+}$ , are predicted to be stabilized by agostic interactions involving the central methylene of the dithiolate. We expect that amine binding would be stronger than an agostic interaction, thus stabilizing this oxidation.<sup>40,41</sup>

(32) Boyke, C. A.; Rauchfuss, T. B.; Wilson, S. R.; Rohmer, M.-M.; Bénard, M. *J. Am. Chem. Soc.* **2004**, *126*, 15151–15160.

(33) Boyke, C. A.; van der Vlugt, J. I.; Rauchfuss, T. B.; Wilson, S. R.; Zampella, G.; De Gioia, L. *J. Am. Chem. Soc.* **2005**, *127*, 11010–11018.

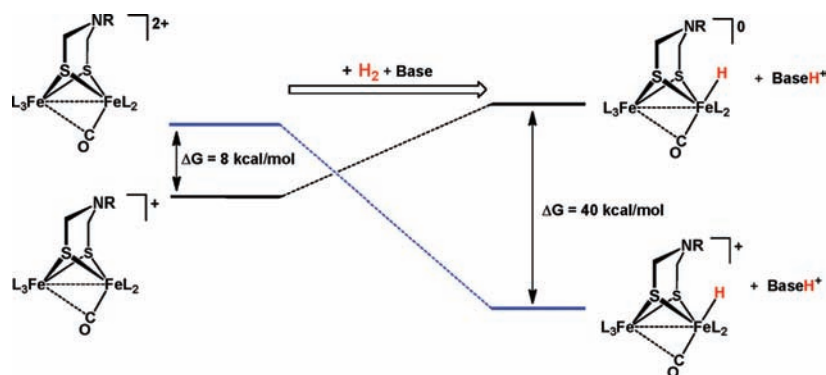


**Figure 6.** Free energy changes (vs  $E(\text{Fc}^{0/+}) = 0$  V) for the hydrogenation of mixed-valence and diferrous dithiolate complexes using data obtained for  $[\text{Fe}_2[(\text{SCH}_2)_2\text{NR}](\text{CO})_3(\text{dppv})(\text{PMe}_3)]^n$  ( $n = +, 2+$ ). The calculation assumes that the proton binds to a base of  $\text{p}K_{\text{a}}^{\text{MeCN}} = 10$ .

**Table 3.** Estimated Affinities of  $[2']^+$  for  $\text{H}^+$ ,  $\text{H}^\bullet$ , and  $\text{H}^-$  (kcal/mol) in MeCN Solution (20 °C)

$\Delta G(\text{H}^+)$	$\Delta G(\text{H}^\bullet)$	$\Delta G(\text{H}^-)$
15	-56	-48

Our measurements suggest that coordination of the amine stabilizes the diferrous state by  $\sim 11$  kcal/mol as indicated by  $\Delta E^{\text{FeII/FeI/FeII/FeI}}$ .

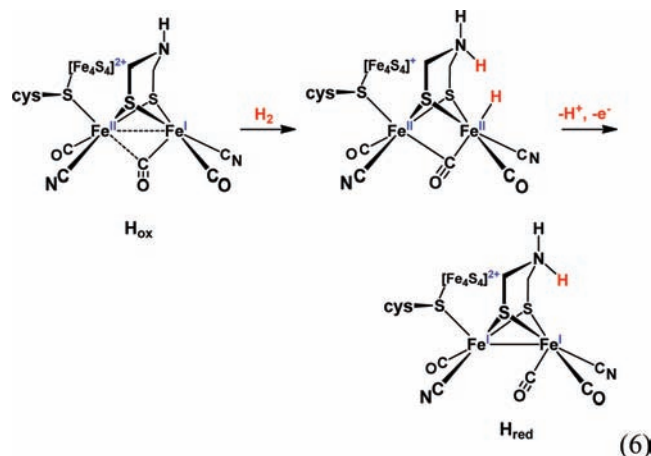
(ii) The  $\text{Fe}^{\text{I}}\text{Fe}^{\text{I}}$  ammonium center serves as an efficient H-atom donor, with concomitant Fe-centered redox. This finding demonstrates the ability of hydrogenase models and, by implication, the enzyme to participate in proton-coupled electron transfer (PCET).

(iii) The basicity of the amine is highly sensitive to the oxidation state of the underlying diiron centers.

The  $[\text{FeFe}]$ -hydrogenases are characterized by reduced and oxidized states, respectively,  $\text{H}_{\text{red}}$  and  $\text{H}_{\text{ox}}$ , that differ by  $1e^-$ . In terms of enzyme mechanism, the reduced state activates protons and the oxidized state activates  $\text{H}_2$ . The oxidation state for the diiron center in  $\text{H}_{\text{red}}$  remains uncertain but is likely either a diferrous hydride or a disubferrous ammonium, which would be readily interconverted.<sup>6</sup> As we demonstrated in this work,  $\text{H}_{\text{red}}$  and  $\text{H}_{\text{ox}}$  are separated formally as well as operationally by  $\text{H}^+$ .

Our measurements bear on the mechanism for activation of  $\text{H}_2$ . In the heterolytic pathway, which is assumed for all hydrogenases,<sup>26</sup>  $\text{H}_2$  is a source of  $\text{H}^-$ , invariably bound to an  $\text{Fe}(\text{II})$ , and  $\text{H}^+$ , which is usually bound to an organic base. We show that the binding of hydride to  $\text{Fe}(\text{II})\text{Fe}(\text{I})$  complexes is far less favorable than that to  $\text{Fe}(\text{II})\text{Fe}(\text{II})$  derivatives (Figure 6). The hydride acceptor strength of  $[2']^+$ ,  $-48$  kcal/mol, is insufficient to compensate for the energy required for the heterolysis of  $\text{H}_2$  (Table 3). Thus  $\text{H}_2$  activation by  $[2']^+$  is predicted to be unfavorable, even when coupled to the neutralization of the proton by a moderately strong base.

The hydride acceptor strength of the diferrous center, e.g.,  $[2']^{2+}$  (assuming  $\kappa^2$ -adt),  $-88$  kcal/mol, is sufficiently exergonic that  $\text{H}_2$  heterolysis is favorable. No biophysical evidence exists, however, for an unsaturated diferrous state for the enzyme. In fact, Nature might avoid this state because it would be unstable with respect to coordination of the amine. The  $2e^-$  change required for exergonic  $\text{H}_2$  activation can however proceed via a PCET pathway,<sup>42</sup> avoiding formation of the Lewis acidic diferrous state. In this scenario, the appended  $4\text{Fe}-4\text{S}$  cluster is poised to provide the oxidizing equivalent (eq 6). PCET has recently been proposed for other hydrogen redox reactions.<sup>3</sup>



The relevance of PCET pathways is reinforced by the facile transfer of  $\text{H}^+$  from the ammonium and hydride tautomers of the diiron dithiolates,  $[\text{Fe}_2[(\text{SCH}_2)_2\text{NHR}](\text{CO})_3(\text{dppv})(\text{PMe}_3)]^+$  and  $[\text{HFe}_2(\text{SR})_2(\text{CO})_2(\text{dppv})_2]^+$ , respectively.

The  $\kappa^3$ -aminodithiolate ligand may be relevant to recent observations on the  $[\text{FeFe}]$ -hydrogenases: upon being oxidized at  $\sim 0$  V (vs SHE), the enzyme from *Desulfovibrio desulfuricans* reversibly deactivates to a state that is protected against oxidative (aerobic) damage.<sup>43,44</sup> It is assumed that this protection is provided by a ligand that occupies the apical site on the distal

(34) van der Vlugt, J. I.; Rauchfuss, T. B.; Whaley, C. M.; Wilson, S. R. *J. Am. Chem. Soc.* **2005**, *127*, 16012–16013.

(35) Geiger, W. E.; Barriere, F. *Acc. Chem. Res.* **2010**, *43*, 1030–1039.

(36) Heiden, Z. M.; Rauchfuss, T. B. *J. Am. Chem. Soc.* **2009**, *131*, 3593–3600.

(37) Li, T.; Lough, A. J.; Morris, R. H. *Chem.—Eur. J.* **2007**, *13*, 3796–3803.

(38) Anelli, P. L.; Biffi, C.; Montanari, F.; Quici, S. *J. Org. Chem.* **1987**, *52*, 2559–2562.

(39) Sen, V. D.; Golubev, V. A. *J. Phys. Org. Chem.* **2008**, *22*, 138–143.

(40) Bruschi, M.; Fantucci, P.; De Gioia, L. *Inorg. Chem.* **2003**, *42*, 4773–4781.

(41) Geiger, W. E.; Ohrenberg, N. C.; Yeomans, B.; Connelly, N. G.; Emslie, D. J. *J. Am. Chem. Soc.* **2005**, *125*, 8680–8688.

(42) Mayer, J. M. *Annu. Rev. Phys. Chem.* **2004**, *55*, 363–390.

(43) Vincent, K. A.; Parkin, A.; Lenz, O.; Albracht, S. P. J.; Fontecilla-Camps, J. C.; Cammack, R.; Friedrich, B.; Armstrong, F. A. *J. Am. Chem. Soc.* **2005**, *127*, 18179–18189.

(44) van Dijk, C.; van Berkel-Arts, A.; Veeger, C. *FEBS Lett.* **1983**, *156*, 340–344.



Fe. Although this blocking ligand might be water or hydroxide,<sup>2,43</sup> the amine could also serve this protective role.

## Materials and Methods

Synthetic methods for  $Fe_2[(SCH_2)_2NBn](CO)_3(dppv)(PMe_3)$  have been recently described.<sup>9</sup> In situ IR measurements employed a React-IR 4000 (Mettler-Toledo). Compounds **1**,<sup>45</sup> **2**,<sup>45</sup> **2'**,<sup>9</sup> **3**,<sup>9</sup>  $FcBAR^F_4$ ,<sup>46</sup> and  $H(OEt_2)_2BAR^F_4$ <sup>47</sup> were prepared as previously reported. 2,2,6,6-Tetramethylpiperidine 1-oxyl (TEMPO) and  $Cp^*_2Co$  were purchased from Sigma Aldrich and sublimed before use. Rate constants were obtained by simulation of experimental data using the program Kintecus.<sup>48</sup>

**Protonation of  $[Fe_2[(SCH_2)_2NBn](CO)_3(dppv)(PMe_3)]BAR^F_4$ .** To a solution of 0.025 g (0.029 mmol) of **2'** in 5 mL of  $CH_2Cl_2$  was added a solution of 0.030 g (0.029 mmol)  $FcBAR^F_4$  in 5 mL of  $CH_2Cl_2$ . The resulting purple solution was thermally equilibrated in an acetone/ $CO_2$  bath for 10 min. A solution of 0.014 g (0.015 mmol) of  $H(OEt_2)_2BAR^F_4$  in 2 mL of  $CH_2Cl_2$  was added to the reaction mixture. The solution immediately became orange in color, and the IR spectrum indicated the presence of only  $[2'](BAR^F_4)_2$  and  $[H2']BAR^F_4$  (see Figure 5). The presence of  $[H2']^+$  was confirmed by allowing it to isomerize to its  $\mu$ -H counterpart. Upon warming to 20 °C, the reaction mixture was filtered through Celite, and the high-field  $^1H$  NMR spectrum ( $CD_2Cl_2$ ) confirmed the presence of  $[2'(\mu-H)]^+$ . Under analogous conditions, a solution of  $[1]BAR^F_4$  in  $CH_2Cl_2$  was shown by IR spectroscopy to be unaffected by the addition of  $H(OEt_2)_2BAR^F_4$ , even after warming to 25 °C.

**$[Fe_2[(SCH_2)_2NBn](CO)_3(dppv)(PMe_3)](BAR^F_4)_2$ .** Into a J. Young NMR tube containing 0.010 g (0.012 mmol) of **2'** and 0.025 g (0.023 mmol) of  $FcBAR^F_4$ , immersed in liquid  $N_2$ , was distilled 1 mL of  $CD_2Cl_2$ . The frozen mixture was thawed in an acetone/ $CO_2$  bath and mixed, with care not to let the contents leave the cold bath. The tube was then quickly inserted into a spectrometer probe precooled to -70 °C. Several hundred scans were necessary for a well-resolved spectrum, possibly owing to the low solubility of the salt.  $^{31}P$  NMR ( $CD_2Cl_2$ , -70 °C):  $\delta$  77.0 (s, dppv), 44.1 (s,  $PMe_3$ ). Upon warming the sample, the spectrum became complex (see Supporting Information).

**$[Fe_2[(SCH_2)_2NBn](CO)_3(dppv)(PMe_3)(CD_3CN)](BAR^F_4)_2$ .** A solution of  $[2'](BAR^F_4)_2$  in  $CD_2Cl_2$  was generated in a J. Young NMR tube as described above. The solution was frozen and re-evacuated, and onto it was distilled 0.1 mL of  $CD_3CN$ . The tube was thawed in an acetone/ $CO_2$  bath and reinserted into the probe, which was precooled to -70 °C.  $^{31}P$  NMR ( $CD_2Cl_2$ , -70 °C):  $\delta$  73.5 (d, dppv,  $J_{P-P} = 11$  Hz, isomer A), 73.0 (s, dppv, isomer A), 20.8 (d,  $J = 11$  Hz,  $PMe_3$ , isomer A). Chemical shifts vary slightly from the isolated complex due to change in counterion ( $BF_4^-$  vs  $BAR^F_4^-$ ). ESI-MS:  $m/z$  432.9  $[Fe_2[(SCH_2)_2NBn](CO)_3(dppv)(PMe_3)]^{2+}$ , 454.9  $[Fe_2[(SCH_2)_2NBn](CO)_3(dppv)(PMe_3)(CD_3CN)]^2$ , 619.4  $[FeCl(CO)_2(dppv)(PMe_3)]^+$ , 900.7  $[Fe_2[(SCH_2)_2NBn]Cl(CO)_3(dppv)(PMe_3)]^+$ .

**$Fe_2[(SCH_2)_2NBn](CO)_4(dppv)(PMe_3)](BAR^F_4)_2$  ( $[2'CO](BAR^F_4)_2$ ).** A solution of  $[2'](BAR^F_4)_2$  in  $CD_2Cl_2$  was generated in a J. Young valve NMR tube as described above. The solution was frozen, and the tube was evacuated and then pressurized with 1 atm of  $CO$ . The tube was thawed in an acetone/ $CO_2$  bath and then slowly warmed to 20 °C.  $^{31}P$  NMR ( $CD_2Cl_2$ , 20 °C):  $\delta$  68.4 (m, dppv), 68.2 (m, dppv), 15.7 (d,  $J = 11$  Hz,  $PMe_3$ ). ESI-MS:  $m/z$  446.9  $[Fe_2[(SCH_2)_2NBn](CO)_4(dppv)(PMe_3)]^{2+}$ , 619.4  $[FeCl(CO)_2(dppv)(PMe_3)]^+$ , 900.7  $[Fe_2[(SCH_2)_2NBn]Cl(CO)_3(dppv)(PMe_3)]^+$ .

**Hydrogenation of  $[2'](BAR^F_4)_2$ .** A solution of  $[2'](BAR^F_4)_2$  was generated by the addition of 5 mL of  $CH_2Cl_2$  to a mixture of 0.025 g (0.029 mmol) of **2'** and 0.064 g (0.058 mmol) of  $FcBAR^F_4$  at 20 °C. The solution of  $[2'](BAR^F_4)_2$  was pressurized (Parr bomb) with 1800 psi  $H_2$  for 30 h to give  $[2'(\mu-H)]^+$  (~50%) and  $[Fe(H)(CO)_3(dppv)]^+$  (~15%) as verified by  $^{31}P$  and  $^1H$  NMR analysis.<sup>49</sup>

**Treatment of  $[2'](BAR^F_4)_2$  with  $PhSiH_3$ .** A mixture of 0.050 g (0.058 mmol)  $[2'](BAR^F_4)_2$  and 0.121 g (0.116 mmol)  $FcBAR^F_4$  was cooled in an acetone/ $CO_2$  bath, and to it was added 2 mL of  $CH_2Cl_2$ . In situ IR spectra indicated the presence of  $[2'](BAR^F_4)_2$ . IR ( $CH_2Cl_2$ ): 2066, 2008, 1977. To this mixture was added 0.2 mL of  $PhSiH_3$ . After ~30 min, the  $[2'](BAR^F_4)_2$  had been consumed. After warming to 20 °C, the sample was found to be spectroscopically ( $^{31}P$  and  $^1H$  NMR, IR, ESI-MS) identical to  $[Fe_2(\mu-H)[(SCH_2)_2NBn](CO)_3(dppv)(PMe_3)]BAR^F_4$ .<sup>9</sup>

**Oxidation of  $[Fe_2[(SCH_2)_2N(H)R](CO)_3(dppv)(PMe_3)]BAR^F_4$  with TEMPO (R = H, Bn).** A solution of  $[2'H]BAR^F_4$  was generated at -78 °C by the addition of 0.8 mL of  $CH_2Cl_2$  to a mixture of 0.023 g (0.027 mmol) of **2'** and 0.027 g (0.027 mmol) of  $H(OEt_2)_2BAR^F_4$ . Treatment of this solution with 0.103 g (0.66 mmol) of TEMPO gave  $[2']^+$ . Similar spectra were obtained using  $[2H]^+$  in place of  $[2'H]^+$ . We independently confirmed by IR spectroscopy that  $[2'H]^+$  was fully deprotonated by 1 equiv of TEMPOH, the organic product of the H-atom transfer reaction (see eq 3). In a related experiment, we found that exposure of a solution of TEMPOH and  $[2'H]^+$  to air rapidly gave  $[2']^+$ . Precautions were taken to avoid this facile aerobic oxidation pathway.

**$[Fe_2[(SCH_2)_2NBn](CO)_3(dppv)(PMe_3)(MeCN)](BF_4)_2$ .** Obtaining single crystals of salts derived from  $[2']^{2+}$  proved challenging. Various counterions ( $BF_4^-$ ,  $SbF_6^-$ ,  $BAR^F_4^-$ , and  $BPh_4^-$ ) and various solvent combinations (slow diffusion at -30 °C of hexanes,  $Et_2O$ , or toluene into  $CH_2Cl_2$  solutions of the respective salts of  $[2']^{2+}$ ) all afforded amorphous tacky solids. We thus turned to the adduct,  $[2'(MeCN)]^{2+}$ . To a Schlenk tube containing a mixture of 0.050 g (0.06 mmol) **2'** and 0.032 g (0.12 mmol) of  $FcBF_4$ , cooled to -78 °C, was added 8 mL of  $CH_2Cl_2$ . The solution was stirred vigorously for 5 min, and then 0.1 mL of MeCN was added. Stirring was stopped, and 40 mL of hexane was carefully layered on top of the reaction mixture and allowed to diffuse at -30 °C. After ~4 days, red crystals had formed. The supernatant was filtered off to remove ferrocene and then the crystalline solid was scrapped from the flask. Finally, this material was dried *in vacuo*, extracted into 5 mL of  $CH_2Cl_2$ , filtered through Celite, and precipitated as an orange-colored powder upon the addition of 20 mL of hexanes. IR ( $CH_2Cl_2$ ,  $cm^{-1}$ ):  $\nu_{CO} = 2065, 2042, 2001, 1974$ .  $^{31}P$  NMR ( $CD_2Cl_2$ , 20 °C):  $\delta$  73.0 (s, dppv, isomer A), 72.9 (d, dppv,  $J_{P-P} = 13$  Hz, isomer A), 21.3 (d,  $J = 13$  Hz,  $PMe_3$ , isomer A).  $^{31}P$  NMR ( $CD_2Cl_2$ , 48 h at 20 °C):  $\delta$  79.9 (s, dppv, isomer B), 25.8 (s,  $PMe_3$ , isomer B). MS ESI:  $m/z = 453.2$  ( $[Fe_2[(SCH_2)_2NBn](CO)_3(dppv)(PMe_3)(MeCN)]^{2+}$ ). The dppv P-Fe-P coupling is not resolved ( $J < 5$  Hz), instead the dppv signal is broadened (FWHM = 14 Hz). Anal. Calcd (Found) for  $C_{43}H_{45}B_2F_8Fe_2N_2O_3P_3S_2$ : C, 47.81 (47.09); H, 4.20 (4.41); N, 2.59 (2.40).

Single crystals were obtained from 8 mL of  $CH_2Cl_2$  solution of 7 mM  $[2'](BF_4)_2$ , which was generated at -78 °C as described above and then treated with 5 drops of MeCN. The solution was then layered with 50 mL of hexane and stored at -30 °C. After 1 week, several red crystals had appeared. Alternatively, a 7 mM solution of  $[2']BF_4$  was treated with 1 drop of MeCN and then layered with 50 mL of hexane. After 1 week, a single cluster of red crystals had formed and were separated from the dark brown solution.

**Crystallography.** Structure was phased by dual space methods. Systematic conditions suggested the ambiguous space group  $P\bar{1}$ . The space group choice was confirmed by successful convergence of the

(45) Justice, A. K.; Zampella, G.; De Gioia, L.; Rauchfuss, T. B.; van der Vlugt, J. I.; Wilson, S. R. *Inorg. Chem.* **2007**, *46*, 1655–1664.

(46) Le Bras, J.; Jiao, H.; Meyer, W. E.; Hampel, F.; Gladysz, J. A. *J. Organomet. Chem.* **2000**, *616*, 54–66.

(47) Brookhart, M.; Grant, B.; Volpe, A. F., Jr. *Organometallics* **1992**, *11*, 3920–3922.

(48) Ianni, J. *Kintecus*, V3.962; 2010.

(49) Sowa, J. R., Jr.; Zanotti, V.; Facchin, G.; Angelici, R. J. *J. Am. Chem. Soc.* **1992**, *114*, 160.

full-matrix least-squares refinement on  $F^2$ . The highest peak in the final difference Fourier map was located 2.6 Å from the nearest aromatic H atom. This residual density located in a void suggests the possibility of a partially occupied water solvate. The final map had no other significant features. A final analysis of variance between observed and calculated structure factors showed no dependence on amplitude or resolution. The proposed model includes two disordered positions for phenyl ring C20–25 of the host cation and two disordered positions for one of two  $\text{CH}_2\text{Cl}_2$  solvate molecules. Phenyl rings were refined as rigid, idealized groups. A common geometry was imposed on the disordered  $\text{CH}_2\text{Cl}_2$  solvates using effective standard deviations of 0.01 and 0.02 Å for bond lengths and bond angles, respectively. Rigid-bond restraints (esd 0.01) were imposed on displacement parameters for all disordered sites, and similar displacement amplitudes (esd 0.01) were imposed on disordered sites overlapping by less than the sum of van der Waals radii. Methyl H atom positions were optimized by rotation about R–C bonds with idealized C–H, R–H and H•••H distances. Remaining H atoms were included as riding idealized contributors. Methyl H atom  $U$ 's were assigned as 1.5 times  $U_{\text{eq}}$  of the carrier atom; remaining H atom  $U$ 's were assigned as 1.2 times carrier  $U_{\text{eq}}$ .

**Electrochemistry.** Cyclic voltammetry experiments were carried out in a ~10 mL scintillation vial inside of a glovebox. The working electrode was a glassy carbon disk (0.3 cm in diameter), the pseudoreference electrode Ag wire, and the counter electrode Pt wire. Under our conditions ( $\text{CH}_2\text{Cl}_2$  solution), we generally observed that  $\Delta E_p$  was ~0.12 V for the  $[\text{Fe}_2]^{0/+}$  couple, whereas an equimolar internal standard of Fc displayed  $\Delta E_p$  as ~0.1 V. Potentials were referenced vs the 0.001 M internal Fc standard.

**Acknowledgment.** This research was sponsored by NIH. M.T.O. thanks the NIH for a CBI-Fellowship.

**Supporting Information Available:** Crystallographic information file (cif) for  $[\mathbf{2}'(\text{MeCN})](\text{BF}_4)_2$ , thermodynamic calculations, and associated spectra. This material is available free of charge via the Internet at <http://pubs.acs.org>.

JA103998V